Top Catal (2011) 54:1392–1402
DOI 10.1007/s11244-011-9766-y

ORIGINAL PAPER

Electrooxidation of D- and L-Glucose at Well-Defined Chiral Bimetallic Electrodes

Omar A. Hazzazi · Catherine A. Harris · Peter B. Wells · Gary A. Attard

Published online: 15 October 2011

Abstract The electrooxidation of D- and L-glucose at chiral Pt{321}$^{r/s}$ single crystal electrodes modified with Au, Ag and Bi adatoms up to a coverage of one monolayer (ML) is reported. All adatoms investigated are found to selectively decorate kink and step sites. Only at higher coverages is adsorption onto the narrow {111} terrace sites observed for Bi, Ag and Au, consistent with previously reported adsorption behaviour on stepped surfaces vicinal to the {111} plane for chemisorbates exhibiting a lower work function than platinum. However, silver is found to block {111} terrace sites even when Pt step sites are still available on Pt{321}. This behaviour is ascribed to the propensity of silver to undergo place-exchange to form a surface alloy. The selective decoration of chiral kink sites has a profound influence on the voltammetric response of Pt{321} towards glucose electrooxidation. For bismuth adsorption, the electrooxidation current density initially increases and reaches a maximum when bismuth adsorption at {111} terraces commences. This is because the reaction pathways at step/kink sites leading to the formation of adsorbed CO (a surface poison for the clean surface reaction) and other strongly adsorbed intermediates, are either blocked by adsorbed bismuth or their electrooxidation and subsequent removal promoted. Once all step/kink sites are blocked by bismuth, hardly any chiral discrimination can be discerned between r-/s-electrodes towards D-/L-glucose. Silver adsorption does not cause any increase in glucose electrooxidation current density but rather induces a continual attenuation in glucose electrooxidation activity, particular (in contrast to bismuth) electrooxidation current at potentials in excess of 0.35 V. Therefore, unlike for bismuth, the initial glucose adsorption and electrooxidation processes associated with chiral kink sites appear to be preserved even though silver adsorbs at these sites. It is speculated that spontaneous place-exchange of silver with platinum to form a PtAg surface alloy at steps is responsible for this difference in behaviour between silver and bismuth. Finally, gold neither promotes reaction rate nor preserves chiral discrimination and is therefore deduced to act as an inert site blocker (no alloying, no promotion of CO electrooxidation) leading to complete attenuation of glucose electrooxidation current at a coverage of one ML.

Keywords Chiral · Bimetallic · Surfaces · Glucose · Electrooxidation

O. A. Hazzazi · C. A. Harris · P. B. Wells · G. A. Attard (✉)
School of Chemistry, Cardiff University, Main Building, Cardiff CF10 3AT, UK
e-mail: attard@cardiff.ac.uk

1 Introduction

Adsorption of adatoms on foreign metal substrates has been studied extensively [1–6]. In electrocatalysis, the aim is to generate more selective or more active catalysts [7]. Interesting results have been reported when metals are preferentially deposited on stepped surfaces in particular. For example, on platinum electrodes copper [8], tin [9], antimony [10], bismuth [11, 12] and tellurium [11] have all been reported to decorate preferentially the step sites, whereas selenium [11] and sulphur [11] decorate terraces preferentially. Feliu and coworkers [12] rationalised the observed differences in deposition sites by examining the electronic properties of the deposited adatoms, in particular their work function. This has been interpreted by means of a simple model in which partially charged adatoms interact with the dipoles at the step sites [12]. They reported that decoration of the steps is related to the work function

differences between the adatoms and substrate. Thus a lower work function value for the adatom favours the deposition of that adatom on the step (e.g. Bi = 4.22 eV, Pt = 5.7 eV) [13] in such a way that hydrogen adsorption is blocked. Adatoms having a higher work function than platinum (e.g. Se = 5.9 eV) [13] will be preferentially adsorbed on the terraces. Interestingly, recent in situ nanoscale, pulsed-laser experiments performed on Pt{111} electrodes dosed with Pb, Bi, S and Se have confirmed the veracity of this description of the resulting modification of the dipole layer [14]. Such adsorption may occur close to the terrace edge, as deduced from the modification of the energy of hydrogen adsorption on the step [12]. Morgenstern et al. [15] explained qualitatively the observed behaviour by considering the electronic charge density deficiency at the upper part of a step due to the Smoluchowski effect. The lower charge density above the step reduces the repulsive part of the interaction between the platinum and the adsorbed species, resulting in a stronger bond. In [12], it was proposed that a similar mechanism would explain both the adsorption of the more electronegative adatoms on the step edge and those adatoms with lower work function at step bottom sites. In many instances superior electrocatalytic properties to the pure supporting metal have resulted [16–18] and an important example of this behaviour was bismuth adsorption on Pt{111} electrodes which was shown to inhibit the spontaneous formation of the surface poison adsorbed CO from formic acid [19].

In the present study, we wish to exploit this ease of generating bimetallic surfaces by irreversible adsorption [20, 21] to re-examine early work in our laboratory and others related to the enantioselective electrooxidation of D- and L-glucose at well-defined chiral Pt{*hkl*} electrodes [22–28]. From an electrochemical standpoint, D-glucose ($HCO–(CHOH)_4–CH_2OH$) is not the chiral probe of choice because of the complexity of its electrooxidation in aqueous solutions [26, 29, 30]. Glucose oxidation leads to the production of gluconolactone, gluconic and glucaric acids [31]. CO is also produced at the beginning of the electrooxidation which is adsorbed strongly on platinum and blocks surface sites. Thus, a surface poison is produced which inhibits glucose reactions (i.e. all electrolytic activity is quenched [30, 32]). This occurs in the potential range in which glucose is normally electrooxidised, and therefore CO can only be removed at more positive overpotentials. In addition, mechanistic studies have conclusively demonstrated that the initial step of glucose adsorption corresponds to the dehydrogenation of the anomeric carbon atom followed at more positive potentials by δ-glucanolactone formation which then under goes hydrolysis to form gluconic acid [26, 27]. As mentioned previously, adsorbed CO has also been shown to form in a parallel pathway together with other strongly adsorbed intermediates [26, 27]. Hence, the glucose electrooxidation currents at more negative potentials may be ascribed to dehydrogenation/CO formation and currents at more positive potentials to the electrooxidation of strongly adsorbed intermediates which cause self-poisoning of the electrode surface unless oxidatively removed [26, 27].

Noting also that glucose electrooxidation is an extremely structure sensitive reaction [30, 32], it therefore allows for detailed investigation of changes in the electrooxidation voltammetric profile as one changes surface structural parameters, including sensitivity to the sense of chirality exhibited by the surface [25, 33]. We have also demonstrated that such chiral variations may be a consequence of compositional change [24] although the intrinsic chiral discrimination of r- and s-kinked surfaces [28, 34–37] was preserved. Therefore, we now investigate the changes engendered by selective decoration of step and kink sites of a Pt{321} electrode by three markedly different adatoms, Au, Ag and Bi and compare their behaviour towards the enantioselective hydrogenation of D- and L-glucose. In addition to these structural aspects of glucose oxidation, it should be remembered that electrochemical oxidation of organic molecules in general has been intensively studied because the current generated in a fuel cell configuration may be related to the amount of electroactive species present. Hence, a fuel-cell-based sensor incorporating chiral discrimination would have profound implications for electroanalysis and electrosynthesis. The overall aim of the study is to illustrate how the electrochemical surface science approach may be used to demonstrate the intrinsic chirality of certain types of clean metal single crystal surfaces and, for the first time, their surface modified bi-metallic analogues.

2 Experimental

Platinum single crystals were oriented, cut and polished from small single crystal beads (2.5 mm diameter) as described previously [38]. Platinum metals used to manufacture the single crystal electrodes were supplied by Goodfellow Metals Ltd (>99.999% purity). The electrodes were flame-annealed and cooled in a H_2 gas bubbler containing ultra-pure water [39]. It has been shown that this treatment leads to the formation of well-defined surfaces [40]. Electrochemical experiments were carried out in a conventional three-electrode cell with a large Pt counter-electrode and a palladium wire charged with hydrogen was used as a reference electrode in contact with the electrolyte. All electrolytes were prepared using 18.2 MΩ cm Milli-Q water and Suprapur (Aristar) grade H_2SO_4 at a concentration of 0.1 M. All glucose solutions (D- and L-glucose

supplied by Aldrich 99.99 and 99.9% purity respectively) were prepared using the same sulphuric acid electrolyte at a concentration of 5 mM in glucose and allowed to stand for 24 h to allow for mutarotation as described previously [28, 41]. Oxygen was eliminated from the electrochemical cell by bubbling N_2 for 20 min.

Gold, silver and bismuth surface layers, with coverages ranging from submonolayer (ML) to one ML were prepared by spontaneous deposition from 10^{-5} to 10^{-6} M aqueous solutions of $HAuCl_4$, $Ag(ClO_4)$ and $Bi(NO_3)_3$ respectively supplied by Alfa (>99.9% purity). Once the deposition had taken place, the electrode was rinsed with Milli-Q water and transferred to an electrochemical cell where the surface was cycled from 0 to 0.85 V until a stable cyclic voltammetry (CV) was recorded. The absence of adsorbate aqueous ions in the electrolyte assisted in determining gold, silver and bismuth coverage in terms of the fraction of hydrogen-underpotential deposition (H-UPD) sites blocked since neither gold, silver or bismuth electrosorb hydrogen. The immersion in the aqueous solution of adsorbate ions sometimes needed to be repeated several times in order to increase adatom coverage to the required level. All voltammetric data was recorded at a sweep rate of 50 mV s^{-1}.

3 Results and Discussion

3.1 Metal Deposition at Pt{321} Single Crystal Electrodes

Figure 1 shows changes in the CV of Pt{321}in aqueous sulphuric acid electrolyte as a function of increasing bismuth loading. Previous work [12] has demonstrated the propensity of bismuth adatoms to occupy linear step sites and the present investigation supports these earlier findings. Bismuth adsorption is characterized by a gradual attenuation in the H-UPD charge region of the clean surface with both {110} and {100} step sites (peaks at 0.07 and 0.21 V respectively) decreasing as bismuth coverage increases whilst the {111} terrace site at 0.5 V remains unchanged. Noteworthy however is the generation of new H-UPD states just positive of the {100} step peak for Bi coverages up to 0.65 MLs (in terms of fraction of clean surface H-UPD charge blocked). Upon further addition of bismuth, these new states, generated as a consequence of bismuth adsorbed at defect sites are attenuated completely and the growth of bismuth on {111} terraces is signified by the appearance of redox peaks at 0.6 V which are clearly split into two components. The {111} clean surface feature at 0.6 V is seen to become much broader as bismuth coverage exceeds 0.65 MLs. The splitting of the bismuth redox peak into two components is reminiscent of previous

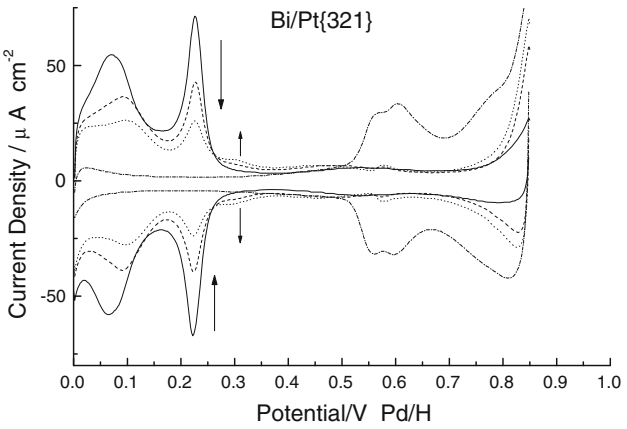

Fig. 1 Voltammetric profiles for consecutive bismuth depositions onto Pt{321}, low-medium coverage (0, 0.35, 0.65 MLs) and high coverage (0.96 MLs). Test solution: 0.1 M H_2SO_4. Sweep rate: 50 mV s^{-1}. *Arrows* indicate change of current density with increasing Bi coverage

work in our group which investigated Bi on Pt{111} electrodes [42]. In that study, the splitting of the bismuth redox peak was ascribed to a change from purely bridge ($(\sqrt{3} \times \sqrt{3})R30°$ phase) to a mixture of atop and multi-fold bismuth adsorption sites as the bismuth coverage exceeded the nominal coverage of 0.33 MLs expected of the $(\sqrt{3} \times \sqrt{3})R30°$ structure. Hence, the formation of a "compressed" hexagonal phase was speculated to lead to a multiplicity of bismuth adsorption sites each possessing its own, specific redox potential. We suggest a similar phenomenon is happening for bismuth adsorbed on the narrow {111} terraces of Pt{321} surface at high bismuth loadings. The increase in intensity of features at potentials >0.7 V is associated with the presence of analogous surface bismuth redox peaks due to bismuth adsorbed at {110} and {100} sites together with bismuth oxidative stripping from the surface at these sites [11]. Hence, potential sweeps positive of 0.85 V were avoided in the present study since the surface coverage of bismuth would be modified by such potential excursions.

Figure 2 shows identical measurements to those depicted in Fig. 1 except bismuth is now replaced with silver. Initial silver adsorption is somewhat similar to bismuth in that gradual attenuation of all H-UPD peaks is observed as a function of increasing coverage. However, some attenuation of the remaining {111} peak is apparent and in fact the {111} site is blocked completely at 0.6 MLs. This behaviour is mostly in accordance with expectations based on differences in work function between silver and platinum [12, 13, 15] although the blocking of {111} sites is unusual. In addition to site blocking, new H-UPD states situated between the potentials of the {100} and {110} step peaks are induced by silver deposition at 0.16 V.

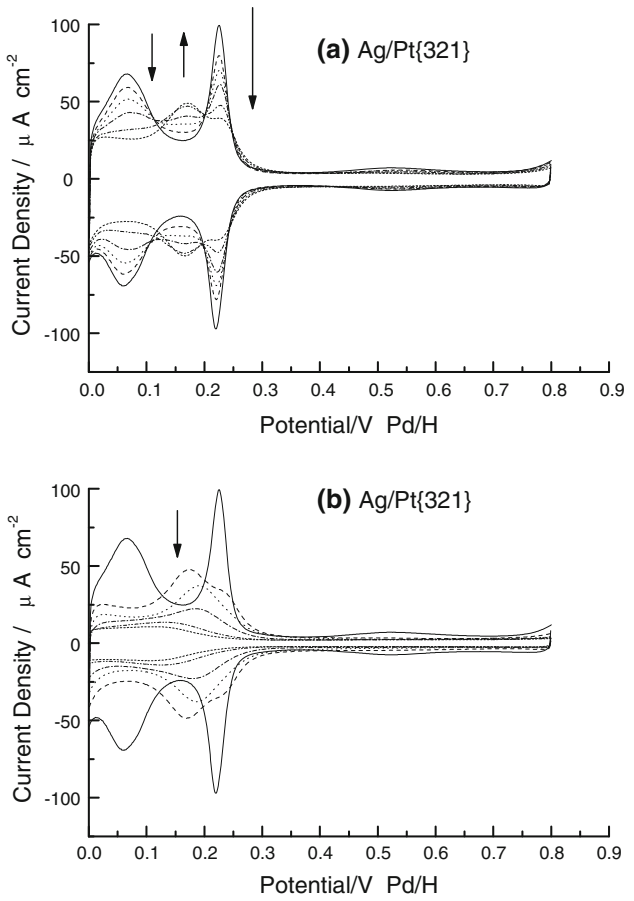

Fig. 2 Voltammetric profiles for consecutive silver depositions to obtain a stable CV onto **a** Pt{321}, low-medium coverage (0, 0.1, 0.2, 0.3, 0.4, 0.5 MLs), **b** Pt{321}, high coverage (0, 0.5, 0.6, 0.75, 0.85, 0.90 MLs). Test solution: 0.1 M H_2SO_4. Sweep rate: 50 mV s^{-1}. *Arrows* indicate change of current density with increasing Ag coverage

These have been noted previously [43, 44] and in this case may be ascribed to partial filling of {110} sites by silver from measurements using Pt{332} electrodes [43, 44]. There is also some intensity generated at potentials just positive of the {100} step site at 0.25 V as found for bismuth and this "shift" in the Pt{100} step peak when silver is adsorbed has also been seen with Pt single crystal electrode surfaces containing linear {100} × {111} steps [44]. It should also be mentioned that Fig. 2 depicts the *stable* CVs obtained after several potential cycles. If the initial CV only is plotted as a function dosing with silver, a response very similar to Fig. 1 is obtained. This indicates that there is a time dependent surface process occurring when silver is adsorbed at Pt. We have already noted the marked tendency for silver to alloy at platinum surfaces [44, 45] and indeed, in both ours and other electrochemical and surface science studies, such a phenomenon is well reported [45–52]. Therefore, we ascribe the generation of new H-UPD states on Pt to be due to place-exchange of silver at step/defect sites forming a surface alloy. These sites may even act as nucleation centres for alloying at terraces [45] and this is thought to explain the differences between silver and bismuth. Silver coverage in excess of 0.5 MLs leads eventually to a single, broad surface alloy H-UPD state at 0.19 V which is gradually attenuated. It proved difficult to place-exchange all Pt atoms of the electrode surface (as signified by the resilience of the H-UPD feature) and the nominal fractional coverage at highest silver loading remained around 0.9.

Figure 3 depicts the behaviour of gold when deposited on Pt{321}. Like bismuth and silver, preferential adsorption at step/defect sites is noted initially although as reported previously [53], there is a greater tendency for gold to adsorb on {111} terrace sites even when vacant step sites are available. This behaviour is thought to relate to the much smaller difference in work function between platinum and gold relative to silver/bismuth and platinum reducing the attractive interaction between the step dipole and the polarized gold adatom [53]. In addition, no evidence for the induction of new H-UPD states was discerned from the data. Rather, all H-UPD states are blocked in a systematic fashion and the total decrease in charge was linear as a function of gold dosing. Therefore, we conclude that gold is an inert site blocker, does not undergo surface alloying with platinum at room temperature like silver and adsorbs preferentially, though not exclusively, in step/defect sites. Hence, each metal adatom behaves in its own distinct manner and in the next section, the effect on glucose electrooxidation is monitored.

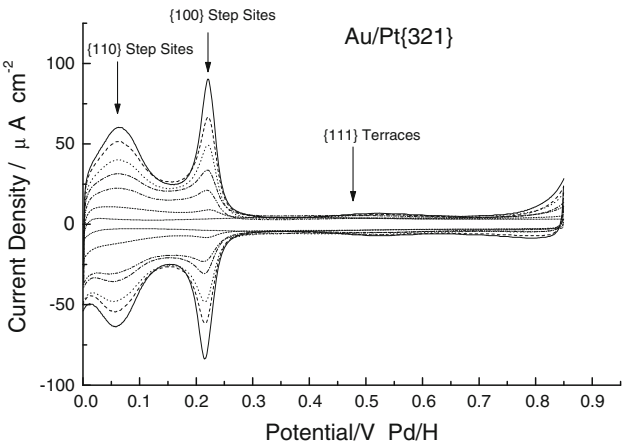

Fig. 3 Voltammetric profiles for consecutive gold depositions onto Pt{321}. Gold coverages = 0, 0.15, 0.33, 0.5, 0.65, 0.77, 0.88, 1.0 MLs. Test solution: 0.1 M H_2SO_4. Sweep rate: 50 mV s^{-1}. Current density decreases with increasing Au coverage

3.2 Electrooxidation of D- and L-Glucose on Clean Pt Chiral Crystals and Their Surface Bimetallic Analogues

3.2.1 Clean Pt{321}$^{r/s}$

Figure 4 shows the first positive going potential sweep of the linear sweep voltammetry (LSV) obtained using Pt{321}$^{r/s}$ chiral electrodes in contact with D- and L-glucose in aqueous sulphuric acid. The result obtained is similar to that reported previously [23, 25, 28] showing a clear diastereomeric response depending on the nature of the glucose being electrooxidised (D- or L-) and the symmetry of the electrode surface.

As described in the introduction, glucose electrooxidation is intrinsically complex but it is possible from previous work to relate the diastereomeric differences recorded to particular adsorption events [26, 27, 30, 32]. The data in Fig. 4 refer to the first, positive going sweep from 0 V. At 0 V, no activity for glucose electrooxidation or electroreduction is observed. Negative of 0.4 V there are three glucose electrooxidation peaks generated although the peak at 0.3 V is absent for the L-/s- and D-/r-diastereomeric combination. This peak has been shown to correspond to the initial dehydrogenation step at {111} terraces [26]. Hence, a strong aspect of the process of chiral discrimination using Pt{*hkl*}$^{r/s}$ electrodes is the ease with which glucose orientates itself with respect to the {111} plane in order to facilitate dehydrogenation and adsorption. In addition, there are two other peaks coincident with the potential of the {110} and {100} step peaks of the clean surface which correspond to the initial dehydrogenation/adsorption reaction at these sites [23]. The {100} step appears to be particularly active for this reaction compared to {110} steps as signified by the large current density observed at 0.2 V relative to 0.07 V and this behaviour has been noted previously [30, 32]. Subsequent potential cycles (not shown) indicate the build-up of site blocking intermediates at steps which greatly diminishes the chiral response compared to the pristine, clean Pt{321} electrode of the first LSV. The fundamental differences between the diastereomeric responses depicted in Fig. 4 are determined

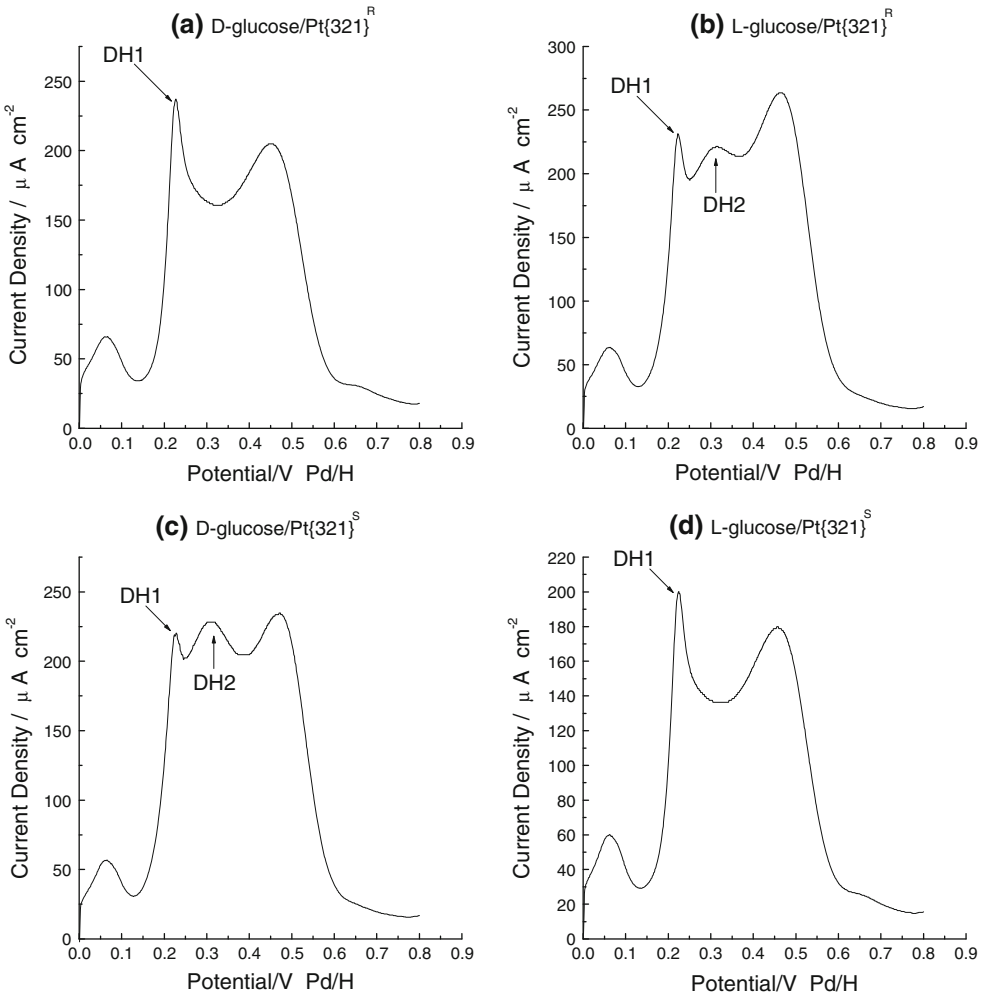

Fig. 4 LSVs for the electrooxidation of 5 mM glucose on Pt{321} in 0.1 M H_2SO_4 at sweep rate 50 mV s^{-1}: **a** D-glucose/Pt{321}^{r}, **b** L-glucose/Pt{321}^{r}, **c** D-glucose/Pt{321}^{s}, **d** L-glucose/Pt{321}^{s}. DH1 and DH2 peaks are indicated (see text)

by the relative activities (current densities) associated with dehydrogenation at {100} step (denoted DH1) and dehydrogenation at {111} terrace sites (denoted DH2). From inspection of Fig. 4, it is evident that:

(i) D-glucose + Pt{321}^{s} and L-glucose + Pt{321}^{r} give the same voltammetry with

DH2 > DH1

(ii) D-glucose + Pt{321}^{r} and L-glucose + Pt{321}^{s} give the same voltammetry with

DH1 > DH2

It is difficult to ascribe a clear, single process to the broad single peak observed at potentials >0.35 V except to say that it appears to correspond to both electrooxidation of strongly adsorbed intermediates of glucose and deeper electrooxidation of glucose itself, perhaps with some CO electrooxidation as well [26, 27, 30, 32].

In fact a further, very small peak at 0.65 V can be discerned particularly for the D-/r- and L-/s-combination which is very reminiscent of CO electrooxidation on platinum electrodes. In the present study, we simply note that such processes of fragment electrooxidation and deeper glucose oxidation may be readily delineated from the initial dehydrogenation/adsorption steps occurring at more negative potentials.

3.2.2 *Bi/Pt{321}$^{r/s}$*

Figure 5 shows changes in glucose electrooxidation LSV as a function of bismuth coverage. For both Pt{321}^{r} and Pt{321}^{s}, the {110} step D- and L-electrooxidation current density at 0.07 V is seen to gradually decrease in size as bismuth coverage increases until all activity is quenched as {111} terrace sites begin to be occupied by bismuth (coverages >0.65 MLs). A similar trend is found for the {100} step peak at 0.22 V although interpretation is complicated by the enormous changes taking place with the initial {111} dehydrogenation peak at 0.3 V and the peak corresponding to electrooxidation of strongly adsorbed molecular fragments which both increase in magnitude significantly. Hence, it is deduced that blocking of step sites by bismuth promotes glucose electrooxidation at residual {111} terraces. This also leads to a remarkable switch in the

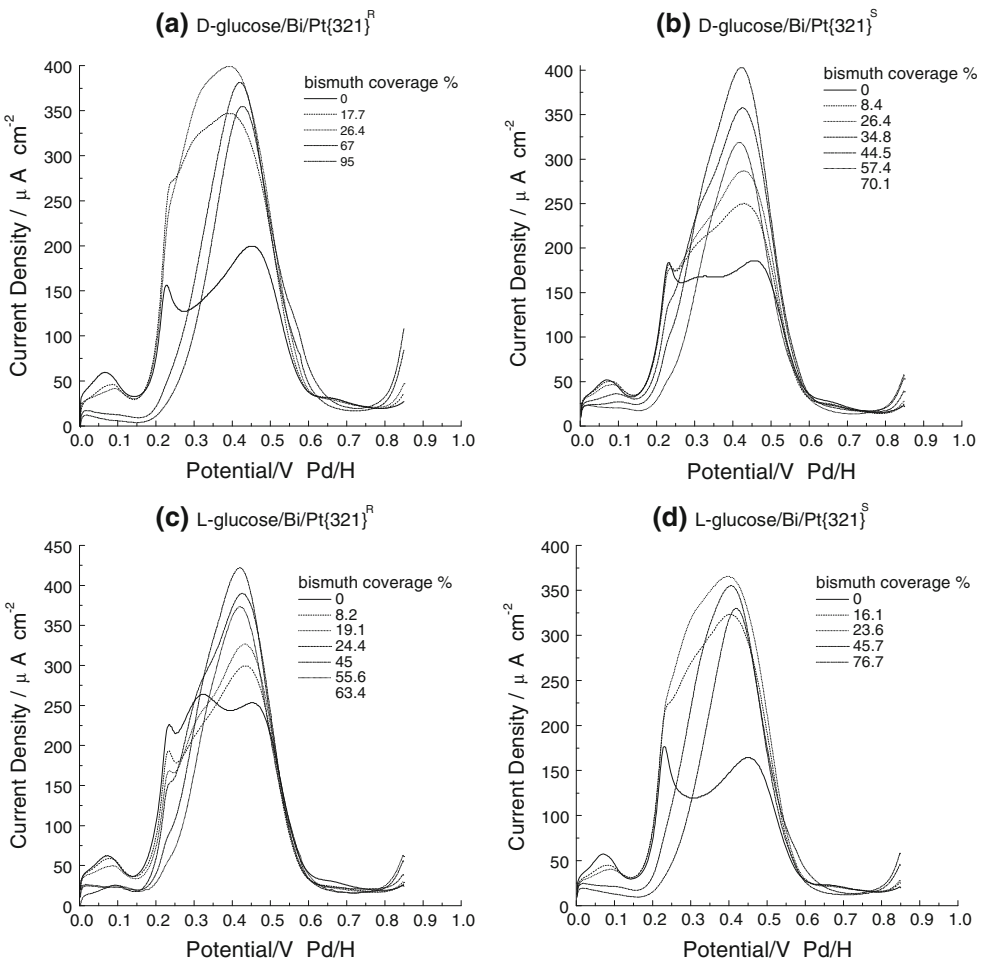

Fig. 5 LSVs for the electrooxidation reaction of 5 mM glucose on Bi-decorated Pt{321} in 0.1 M H_2SO_4 at sweep rate of 50 mV s^{-1}: **a** D-glucose/Bi/Pt{321}^{r}, **b** D-glucose/Bi/Pt{321}^{s}, **c** L-glucose/Bi/Pt{321}^{r}, and **d** L-glucose/Bi/Pt{321}^{s}

relative magnitudes of DH1 and DH2 contributions with a clear DH2 peak now being observed in both the D-/r- and L-/s-combinations for bismuth coverages <50% where absolutely no peak was observed previously for the clean surface. Interestingly, for the D-/s- and L-/r-combination, a diminution in DH2 contribution is observed in the same range of bismuth coverage. In both cases, the DH1 contribution is gradually attenuated until when all step sites are blocked, only the peak corresponding to electrooxidation of strongly adsorbed intermediates remains. Crucially, at this stage, there appears to be no chiral discrimination at all and every Pt{321} LSV is similar irrespective of the D-/L-/r-/s-combination. Hence, in contrast to clean platinum, for bismuth coverages between 0 and 0.6 MLs:

(i) D-glucose + Pt{321}^{s} and L-glucose + Pt{321}^{r} give the same voltammetry with

$$DH2 < DH1$$

(ii) D-glucose + Pt{321}^{r} and L-glucose + Pt{321}^{s} give the same voltammetry with

$$DH1 < DH2$$

3.2.3 *Ag/Pt{321}$^{r/s}$*

Figure 6 shows the diastereomeric LSV data for glucose electrooxidation for silver-modified Pt{321}. In contrast to bismuth, no promotion of glucose electrooxidation activity is seen. Furthermore, instead of quenching of the dehydrogenation reactions at the various adsorption sites on the electrode surface, the action of silver is initially to inhibit electrochemical reactions occurring at positive potentials associated with strongly adsorbed intermediates. This, together with the overall linear decrease in glucose electrooxidation activity as a function of silver loading, indicates silver adsorbed on platinum clearly acts as a poison. Nonetheless, unambiguous chiral discrimination is being observed even up to the highest Ag coverages ($\sim$0.7 MLs). As mentioned earlier, the ability of the chiral kink sites to maintain an influence on the initial dehydrogenation/adsorption steps of glucose (in contrast to bismuth) must be associated with the presence of Pt surface atoms at such sites due to place-exchange and surface alloy formation. In contrast to bismuth however, there is no switching of the relative magnitudes of DH1 and DH2 as silver coverage

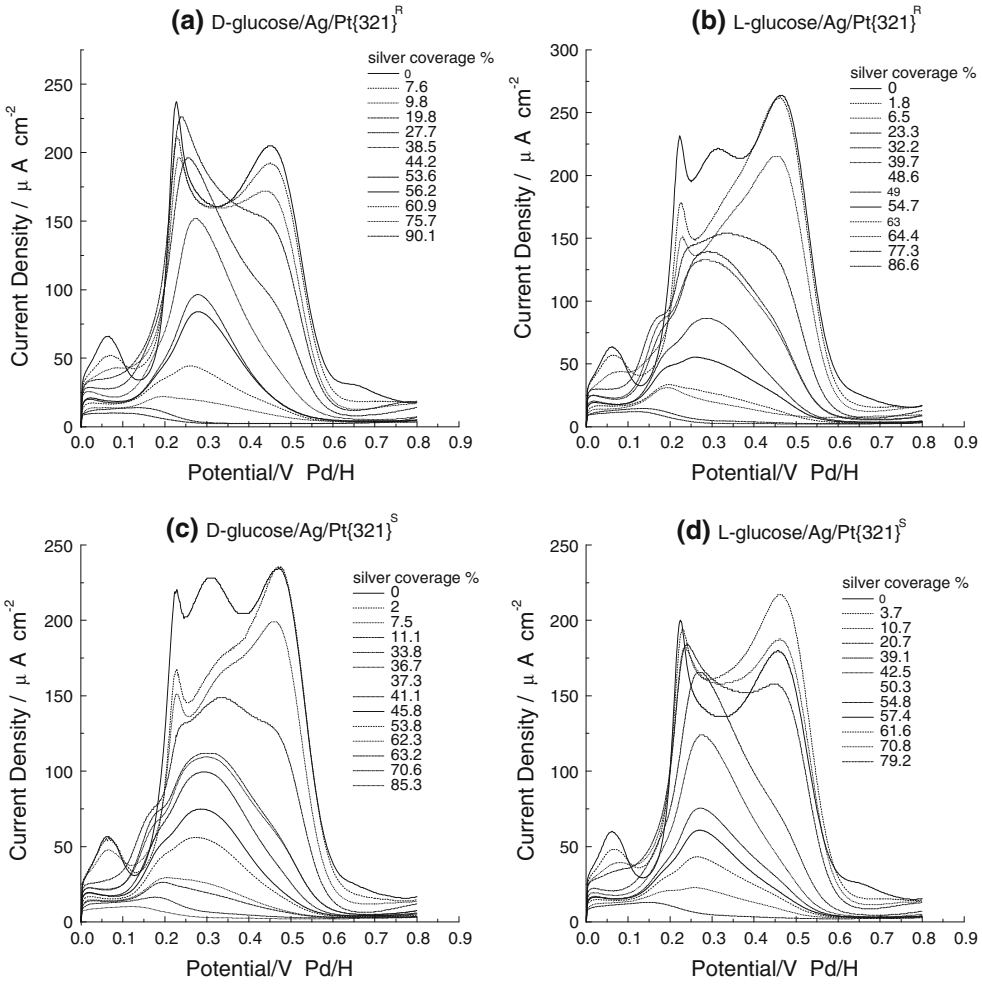

Fig. 6 LSVs for the electrooxidation reaction of 5 mM glucose on Ag-decorated Pt{321} in 0.1 M H_2SO_4 at sweep rate 50 mV s^{-1}: **a** D-glucose/Ag/Pt{321}^{r}, **b** L-glucose/Ag/Pt{321}^{r}, **c** D-glucose/Ag/Pt{321}^{s}, **d** L-glucose/Ag/Pt{321}^{s}

increases. Rather, as for the clean surface Pt{321} electrode:

(i) D-glucose + Ag/Pt{321}^{s} and L-glucose + Ag/Pt{321}^{r} giving the same voltammetry with DH2 > DH1

and

(ii) D-glucose + Ag/Pt{321}^{r} and L-glucose + Ag/Pt{321}^{s} giving the same voltammetry with DH1 > DH2

Also, unlike for bismuth, it is evident from Fig. 6 that the electrooxidation processes positive of 0.35 V, ascribable to electrooxidation of glucose-derived strongly adsorbed intermediates, is almost entirely attenuated as silver coverage increases whereas a measurable dehydrogenation/adsorption intensity between 0 and 0.2 V is always found. Taken together with the contrasting behaviour of silver and bismuth in relation to reactivity towards {111} terrace sites (and the fact that electrooxidation currents at potentials >0.35 V reach a maximum for bismuth when all step/kink sites are blocked), we ascribe this behaviour of silver to the process of silver place-exchange at terrace sites. That is, as soon as Pt{111} terrace sites become blocked by silver, all electrocatalytic activity becomes reduced significantly. This is consistent with previous reports whereby the "narrowing" in average Pt{111} terrace width for clean Pt{*hkl*} electrodes was shown to lead to a remarkable decreases in electrocatalytic activity towards glucose [30].

Figure 7 shows the result of continuous gold adsorption on the electrocatalytic activity of Pt{321} towards glucose electrooxidation. Like silver, a linear decrease in electrooxidation current density as a function of gold coverage is observed although unlike silver, it appears that both the dehydration/adsorption step and electrooxidation of strongly adsorbed intermediates is attenuated equally. In contrast to bismuth as well (but similar to silver) no promotion of glucose electrooxidation is observed for gold. That is, taken overall, no evidence for place-exchange

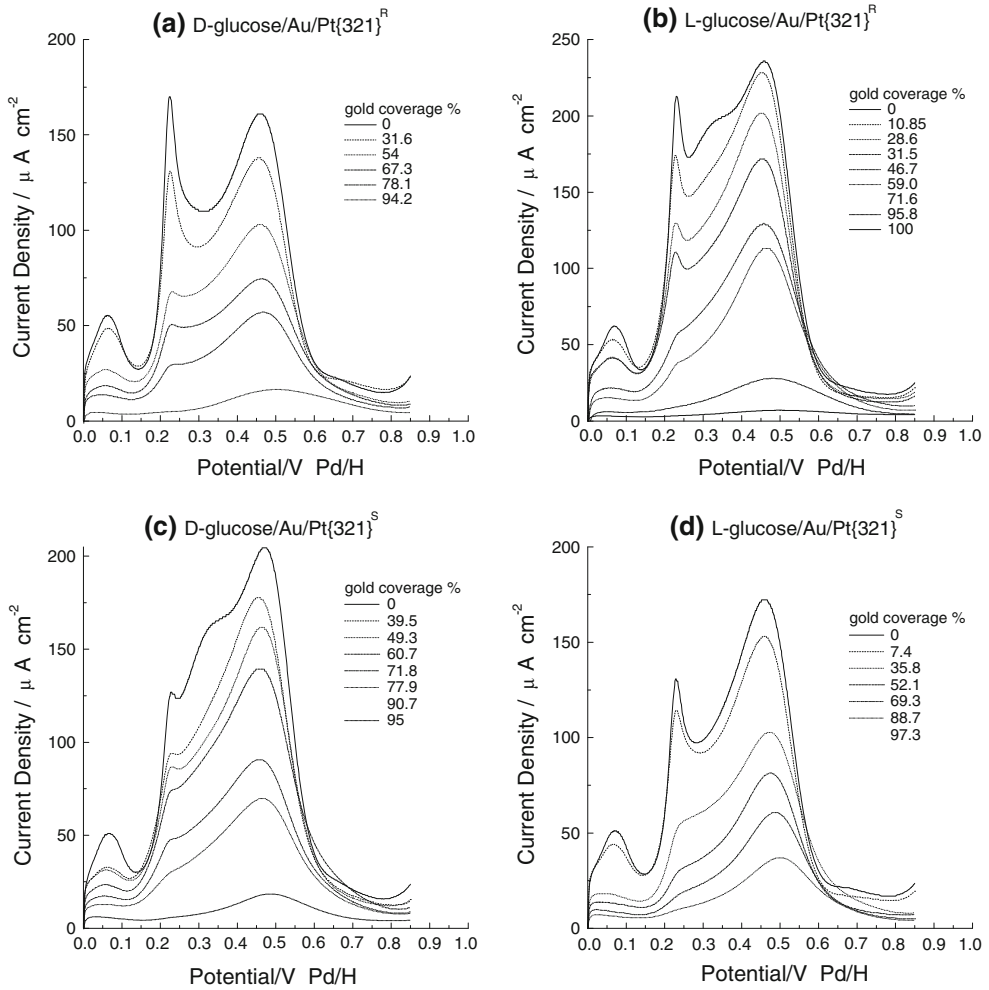

Fig. 7 LSVs for the electrooxidation reaction of 5 mM glucose on Au-decorated Pt{321} in 0.1 M H_2SO_4 at sweep rate 50 mV s^{-1}: **a** D-glucose/Au/Pt{321}^{r}, **b** L-glucose/Au/Pt{321}^{r}, **c** D-glucose/Au/Pt{321}^{s}, **d** L-glucose/Au/Pt{321}^{s}

between gold and platinum is apparent and the gold adatoms appear to be acting as simple site blockers.

This result is consistent with the fact that although gold initially adsorbs at defect sites, it also exhibits some preference for {111} terrace sites even though vacant step sites may still be available [53]. Hence, the blocking of clean surface sites by gold adatoms is much less selective than either bismuth in particular, or silver, leading to an almost non-selective attenuation of the clean surface voltammetry. At around 70% gold coverage all dehydrogenation peaks are weak and only the electrooxidation of glucose-derived strongly adsorbed intermediates at {111} terraces remains.

Minor chiral discrimination may be observed for most gold coverages but it is more subtle than before but similar to the clean surface response. Because of this very weak differentiation, Fig. 8 shows the same measurements as in Fig. 7 but for a still more kinked Pt{531} [54] electrode in order to accentuate the chiral response. Note that overall, electric current densities are smaller for Pt{531} compared to Pt{321} since Pt{531} is ostensibly free of any {111} terrace sites. However, as found for clean Pt{*hkl*} electrode surfaces, the extent of chiral discrimination for the bimetallic gold surface is a function of the surface density of kinks [25].

4 Conclusion

The electrooxidation of D- and L-glucose at chiral Pt{321}$^{r/s}$ single crystal electrodes modified with Au, Ag and Bi adatoms up to a coverage of 1 ML has been investigated. Bi, Ag and Au selectively decorate kink and step sites at low coverages. Only at higher coverages is adsorption onto the narrow {111} terrace sites observed. This behaviour is consistent with previous studies on stepped surfaces vicinal to the {111} plane for chemisorbates exhibiting a lower work function than platinum. However, silver is found to block {111} terrace sites even when Pt step sites are still available. This characteristic response is ascribed to the propensity of silver to undergo place-exchange to form a

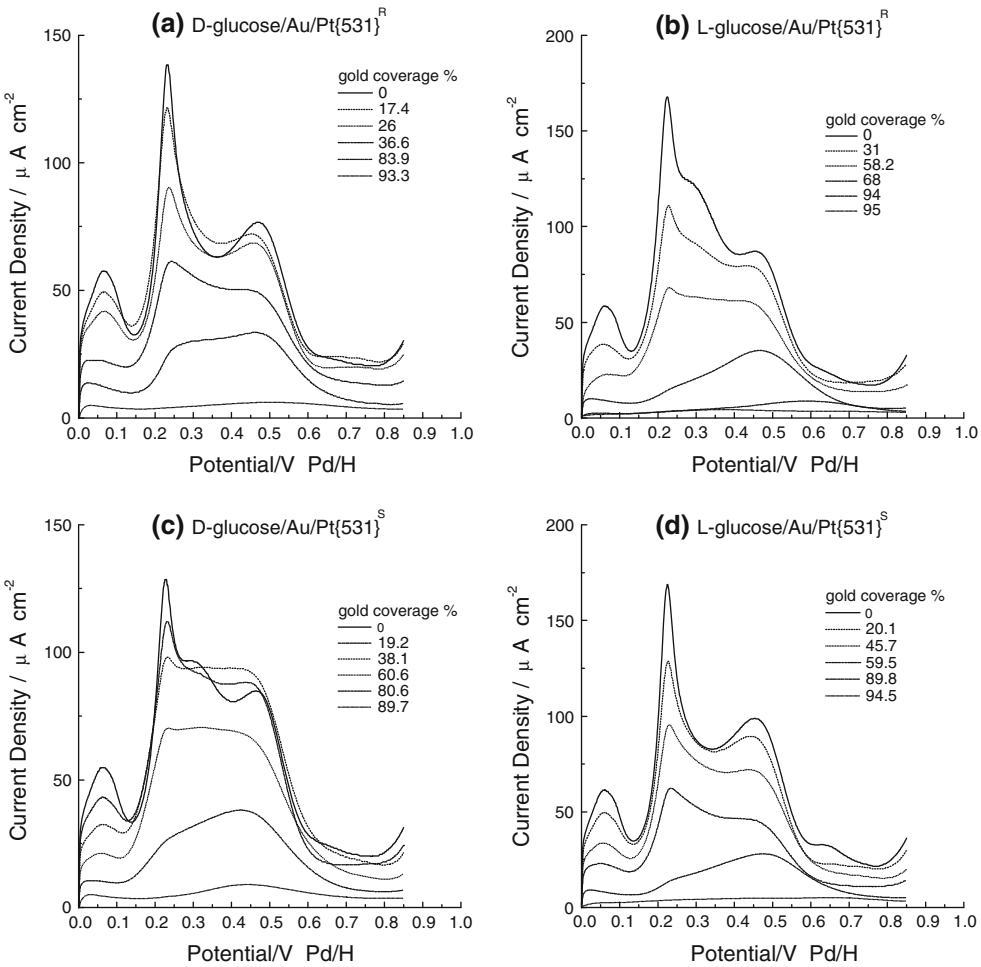

Fig. 8 LSVs for the electrooxidation reaction of 5 mM glucose on Au-decorated Pt{531} in 0.1 M H_2SO_4 at sweep rate 50 mV s^{-1}: **a** D-glucose/Au/Pt{531}^{r}, **b** L-glucose/Au/Pt{531}^{r}, **c** D-glucose/Au/Pt{531}^{s}, **d** L-glucose/Au/Pt{531}^{s}

surface alloy. The selective decoration of chiral kink sites has a profound influence on the LSV of Pt{321} during glucose electrooxidation. For bismuth adsorption, the electrooxidation current density initially increases and reaches a maximum when bismuth adsorption at {111} terraces commences (all step sites occupied). This is because the reaction pathways at step/kink sites leading to the formation of adsorbed CO (a surface poison for the clean surface reaction) and other strongly adsorbed intermediates, are either blocked by adsorbed bismuth or their electrooxidation and subsequent removal promoted. Once all step/kink sites are blocked by bismuth, hardly any chiral discrimination can be discerned towards D-/L-glucose. Silver adsorption does not cause any increase in glucose electrooxidation current density but rather induces a continual attenuation in glucose electrooxidation activity, particular (in contrast to bismuth) electrooxidation current at potentials in excess of 0.35 V. Therefore, unlike for bismuth, the initial glucose adsorption and electrooxidation processes associated with chiral kink sites appear to be preserved even though silver ostensibly adsorbs at these sites. It is speculated that spontaneous place-exchange of silver with platinum to form a PtAg surface alloy at steps is responsible for this difference in behaviour between silver and bismuth. Finally, gold neither promotes reaction rate nor preserves chiral discrimination and is therefore deduced to act as an inert site blocker (no alloying, no promotion of CO electrooxidation) leading to complete attenuation of glucose electrooxidation current at a coverage of one ML.

Acknowledgment The authors would like to thank the EPSRC for financial support. Omar A. Hazzazi expresses his thanks to the Saudi Arabian Government for financial support. GAA acknowledges the help of Sharon Huxter in the preparation of the figures.

References

1. Naohara H, Ye S, Uosaki K (1999) J Electroanal Chem 473:2
2. Kibler LA, Kleinert M, Kolb DM (2000) Surf Sci 461:155
3. Kibler LA, Kleinert M, Lazarescu V, Kolb DM (2002) Surf Sci 498:175
4. Kibler LA, Kleinert M, Randler R, Kolb DM (1999) Surf Sci 443:19
5. Waibel H-F, Kleinert M, Kibler LA, Kolb DM (2002) Electrochim Acta 47:1461
6. Sung Y-E, Chrzanowski W, Wieckowski A, Zolfaghari A, Blais S, Jerkiewicz G (1998) Electrochim Acta 44:1019
7. Rhee CK, Wakisaka M, Tolmachev YV, Johnston CM, Haasch R, Attenkofer K, Lu GQ, You H, Wieckowski A (2003) J Electroanal Chem 554:367
8. Buller LJ, Herrero E, Gomez R, Feliu JM, Abruña HD (1996) J Chem Soc Faraday Trans 92:3757
9. Massong H, Tillmann S, Langkau T, Abd El Meguid EA, Baltruschat H (1998) J Electrochem Acta 44:1379
10. Maciá MD, Herrero E, Feliu JM (2002) Electrochim Acta 47:3653
11. Clavilier J, Feliu JM, Aldaz A (1988) J Electroanal Chem 243:419
12. Herrero E, Climent V, Feliu JM (2000) Electrochem Commun 2:636
13. Michaelson HB (1977) J Appl Phys 48:4729
14. Garcia-Araez N, Climent V, Feliu JM (2008) J Am Chem Soc 130:3824
15. Morgenstern M, Michely T, Comsa G (1996) Phys Rev Lett 77:703
16. Gutiérrez De Dios FJ, Gómez R, Feliu JM (2001) Electrochem Commun 3:659
17. Lei H-W, Hattori H, Kita H (1996) Electrochim Acta 41:1619
18. Yang Y-Y, Sun S-G, Gu Y-J, Zhou Z-Y, Zhen C-H (2001) Electrochim Acta 46:4339
19. Herrero E, Fernández-Vega A, Feliu JM, Aldaz A (1993) J Electroanal Chem 350:73
20. Janssen MMP, Moolhuysen J (1976) Electrochim Acta 21:861
21. Clavilier J, Llorca MJ, Feliu JM, Aldaz A (1991) J Electroanal Chem 310:429
22. Hazzazi OA, Attard GA, Wells PB (2004) J Mol Catal A Chem 216:247
23. Attard GA, Harris C, Herrero E, Feliu J (2002) Faraday Discuss 121:253
24. Watson DJ, Attard GA (2001) Electrochim Acta 46:3157
25. Attard GA (2001) J Phys Chem B 105:3158
26. Popovic KD, Tripkovic AV, Adzic RR (1992) J Electroanal Chem 339:227
27. Beden B, Largeaud F, Kokoh KB, Lamy C (1996) Electrochim Acta 41:701
28. Ahmadi A, Attard G, Feliu J, Rodes A (1999) Langmuir 15:2420
29. Kokkiniois G, Leger JM, Lamy C (1988) J Electroanal Chem 242:221
30. Rodes A, Llorca MJ, Feliu JM, Clavilier J (1996) Anal Quim Int Ed 92:118
31. Marinkovic NS, Popovic KD, Tripkovic AV, Markovic NM, Adzic RR (1992) Proc Electrochem Soc 92:353
32. Llorca MJ, Feliu JM, Aldaz A, Clavilier J, Rodes A (1991) J Electroanal Chem 316:175
33. Martins A, Ferreira V, Queiros A, Aroso I, Silva F, Feliu J (2003) Electrochem Commun 5:741
34. Pratt SJ, Jenkins SJ, King DA (2005) Surf Sci 585:L159
35. McFadden CF, Gremer PS, Gellman AJ (1996) Langmuir 12:2483
36. Sholl DS (1998) Langmuir 14:862
37. Attard GA, Ahmadi A, Feliu J, Rodes A, Herrero E, Blais S, Jerkiewicz G (1999) J Phys Chem B 103:1381
38. Clavilier J, Armand D, Sun SG, Petit M (1986) J Electroanal Chem 205:267
39. Rodes A, Zamakhchari MA, El Achi K, Clavilier J (1991) J Electroanal Chem 305:115
40. Al-Akl A, Attard G, Price R, Timothy B (2001) Phys Chem Chem Phys 3:3261
41. Morrison RT, Boyd RN (1973) Organic chemistry, 3rd edn. Allyn and Bacon, M. A., Boston, p 1095
42. Evans RW, Attard GA (1993) J Electroanal Chem 345:337
43. Domke KF, Xiao XY, Baltruschat H (2009) Electrochim Acta 54:4829
44. Hazzazi OA (2002) Doctoral Thesis, Cardiff University, UK
45. Attard GA, Al-Akl A (2003) J Electroanal Chem 554:439
46. Aberdam D, Salem C, Durand R, Faure R (1990) Surf Sci 239:71
47. Batzill M, Koel BE (2004) Surf Sci 553:50
48. Batzill M, Koel BE (2003) Europhys Lett 64:70
49. Tsay JS, Yao YD, Shern CS (1998) Phys Rev B 58:3609

50. Casalis L, Gunther S, Kovac J, Marsi M, Kiskinova M, Bifone A (1998) Chem Phys Lett 290:245
51. Tsay JS, Shern CS (1996) Chin J Phys 34:130
52. Vaskevich A, Rosenblum M, Gileadi E (1995) J Electroanal Chem 383:167
53. Hazzazi OA, Attard GA, Wells PB, Vidal-Iglesias FJ, Casadesus M (2009) J Electroanal Chem 625:123
54. Clavilier J, Orts JM, Gomez R, Feliu JM, Aldaz A (1996) J Electroanal Chem 404:281